N90-17650

HIGH REYNOLDS NUMBER TESTS OF THE CAST-10-2/DOA 2 TRANSONIC AIRFOIL AT AMBIENT AND CRYOGENIC TEMPERATURE CONDITIONS *

E. Stanewsky and F. Demurie
Deutsche Forschungs- und Versuchsanstalt für Luft- und Raumfahrt e.V.
Institut für Experimentelle Strömungsmechanik
Göttingen, FRG

and

E.J. Ray and C.B. Johnson
National Aeronautics and Space Administration
Langley Research Center, Hampton, Va 23665

*Paper reprinted from AGARD Conference Proceedings No. 348.

SUMMARY

The transonic airfoil CAST 10-2/DOA2 was investigated in several major transonic wind tunnels at Reynolds numbers ranging from Re=1.3 x 10^6 to 45 x 10^6 at ambient and cryogenic temperature conditions. The main objective was to study the degree and extent of the effects of Reynolds number on both the airfoil aerodynamic characteristics and the interference effects of various model-wind-tunnel systems. The initial analysis of the CAST 10-2 airfoil results has revealed appreciable "real" Reynolds number effects on this airfoil and, moreover, shown that wall interference can be significantly affected by changes in Reynolds number thus appearing as "true" Reynolds number effects.

LIST OF SYMBOLS

AR	aspect ratio, B/c
B	tunnel width (model span)
c	airfoil chord
C_D	drag coefficient
C_L	lift coefficient
ΔC_{LL}	deviation from linear lift curve slope
ΔC_{DL}	spanwise drag variation, $C_{DB/2}-C_{DB/4}$
c_p	pressure coefficient, $(p-p_\infty)/q_\infty$
H	tunnel height
M_∞	freestream Mach number
$M_{\infty C}$	corrected freestream Mach number
$M_{\infty D}$	drag-rise Mach number
p	static pressure
q	dynamic pressure
Re	Reynolds number based on freestream conditions and chord
T_S	transonic sensitivity parameter (FIG.1)
x, y, z	Cartesian coordinates (x in chordwise direction)
α	angle of attack

Subscripts

∞	freestream conditions

Abbreviations

SL	slotted
PE	perforated
BLC	boundary layer control
Cts	Counts

I INTRODUCTION

The CAST 10-2/DOA2 airfoil, designed by Dornier, has been shown in previous tests to be extremely sensitive to changes in the initial boundary layer conditions. The high sensitivity of this airfoil compared to other contemporary supercritical type airfoils is demonstrated in FIG.1 where the change in lift with changing transition point location is plotted against the transonic similarity parameter T_S derived in REF.1. Due to this unusual sensitivity, the CAST 10-2 airfoil was selected by the DFVLR and NASA for a cooperative study to consider the following objectives:

- o Assessment of the degree and extent of the effects of Reynolds number on both the aerodynamic characteristics of the airfoil and the interference effects of various model-wind-tunnel systems.

- o Correlation of the results obtained in the Langley 0.3-m Transonic Cryogenic Tunnel (TCT) with results from other major facilities.

- o Evaluation of current analytical and experimental techniques to account for wall interference effects over a wide range of Reynolds numbers.

Since the evaluation of analytical and experimental correction techniques has not yet progressed sufficiently, we will concentrate here on the first two objectives. This paper must, furthermore, be considered as an interim report since the data analysis as well as the experimental program are continuing.

II EXPERIMENTS

The CAST 10-2 airfoil and characteristic airfoil related data are presented in FIG. 2. Further information concerning the airfoil, including design procedures, is given in REF. 2. As shown in TABLE 1, CAST 10-2 airfoil models have been tested in the DFVLR Transonic Wind Tunnel Göttingen (TKG) [3], the DFVLR Transonic Wind Tunnel Braunschweig (TWB) [4], the Lockheed Georgia Compressible Flow Wind Tunnel (CFWT) [5] and the NASA Langley 0.3-m Transonic Cryogenic Tunnel (TCT) [6]. The matrices of model-wind-tunnel system parameters and test conditions considered in the program have been extensive and have included tunnel-height to model-chord ratios ranging from 4 to 8, tunnel-width to model-chord ratios between 1.3 and 5 and slotted and perforated test section walls. In the 0.3-m TCT phase of the studies, two models with chord lengths of 152.4 and 76.2 mm were tested with and without boundary layer control[1] to enable a determination of wall interference effects in the same tunnel as well as by comparisons with results obtained in other test facilities. The study included tests at subsonic and transonic velocities over a large angle-of-attack range. Note, that the overall scope of the study has recently been expanded to include a cooperative effort with the ONERA to test a CAST 10-2 airfoil model provided by that institution in the ONERA T2 and the NASA 0.3-m TCT Cryogenic Self-Streamlining Wall Facilities.

FIG. 3 illustrates the broad two-dimensional Reynolds number and Mach number envelopes provided by the test facilities utilized during the present CAST 10-2 studies. Traditionally, the transport aircraft design trend, shown by the solid curve, has established the upper requirements for airfoil testing. In recent years there has been a dramatic increase in these requirements as illustrated by the design conditions shown for current transport aircraft such as the Airbus and the Boeing 747 and the cargo aircraft envisioned for the not too distant future. As can be seen from FIG. 3, the two-dimensional 0.3-m TCT provides an adequate Reynolds number and Mach number capability to simulate the design flight conditions for current transport aircraft and will provide an even higher Reynolds number capability for the forthcoming CAST 10-2 self-streamlining wall tests.

Both the model-wind-tunnel system and test condition variables considered in the present program have been very extensive. Some of the major effects of these variables will be addressed in the following sections of this paper.

III ANALYSIS OF EXPERIMENTAL RESULTS

The wind-tunnel results obtained with the CAST 10-2 airfoil models have shown some rather surprising and unexpected characteristics. For instance, the extreme sensitivity of the airfoil to tunnel wall effects and, as mentioned in the introduction, the effects due to viscous-inviscid interactions on the airfoil is manifested in what might be considered to be an unusual variation of lift with angle-of-attack at supercritical Mach number conditions. This behavior is illustrated qualitatively in FIG. 4 which shows at the left the typical effects of model-tunnel systems on the variations of lift with incidence at a given Reynolds number. In general, the supercritical lift behavior is here characterized by a low angle-of-attack linear lift variation which is well understood and correctable by approaches suggested, for instance, in REF. 7 and 8. The linear lift region, however, is followed by non-linear lift and flow break-down regions which are highly susceptible to both Reynolds number effects and the complicated effects of the integrated model-wind-tunnel system. In addition, since the various model-wind-tunnel arrangements are affected by changes in boundary layer condition as integrated systems, changes in Reynolds number will affect the wall interference characteristics as well as the aerodynamic characteristics of the airfoil.

Non-linear and flow-break-down regions will be examined in more detail to study the combined effects of model-tunnel system and Reynolds number on the (measured) aerodynamic behavior of the airfoil. Essentially "pure" Reynolds number effects, depicted on the right hand side of this figure, will then be considered at conditions believed to be virtually unaffected by wall interference.

---

[1]) BLC on the sidewalls upstream of the model

COMBINED WALL INTERFERENCE AND REYNOLDS NUMBER EFFECTS

Non-linear lift

Let us first examine in more detail the relationship between the non-linear lift region and the sidewall interference effects of several model-wind-tunnel systems. In FIG. 5 lift has been plotted against angle-of-attack for three different model-wind-tunnel configurations. Lift results are shown for the 152 mm chord airfoil and the 76 mm airfoil in the 0.3-m TCT and for a CAST 10-2 model in the Lockheed CFWT facility. For this case, the models were tested at a supercritical Mach number of 0.73 at a Reynolds number of Re = 10 x 10^6, transition free. The studies have indicated that at this Reynolds number the boundary layer is basically turbulent with a relatively stable transition point located near the leading edge of the airfoils.

It will be noted that there is only a small deviation from a linear lift variation for the large chord TCT model, denoted by circular symbols. This lift behavior might be considered to be normal and expected; however, the small chord TCT and the CFWT airfoils with the substantially higher aspect ratios, i.e. tunnel-breadth to model-chord ratios, show a very pronounced non-linear increase in lift. This comparison suggests that in the case of the large chord, small aspect ratio TCT model, the tunnel sidewall interference effects suppress the non-linear lift increase. This is supported by the spanwise drag distributions which clearly demonstrate the degree of three-dimensional effects due to the interaction with the sidewall boundary layer. The small insert figures indicate the drag levels measured with a "spanwise" wake rake located downstream of the model. The values were measured at stations extending from slightly beyond the centerline of the tunnel to the tunnel sidewall. In the low incidence case, when the lift variation is fairly linear for all of the airfoils, there are only small drag variations across the span of the tunnel. At the higher angles-of-attack, in the area of appreciable divergence in the linear lift behavior large spanwise variations in drag were shown for the large chord TCT model, while the spanwise variation in drag for the small chord TCT airfoil is still quite small. The large drag decreases noted for the large chord model midway between the tunnel wall and centerline are believed to be caused by compression waves originating from the separated sidewall boundary layer which locally reduce the shock losses on the airfoil. The increase in drag shown near the wall of the tunnel suggests that at this condition the separated boundary layer region extends to a point beyond the pitot probe nearest to the wall. Although not as extensive, a similar boundary layer growth process must take place for the smaller model. However, the boundary layer "thickening" process here takes place closer to the wall of the tunnel. Comparing corresponding pressure distributions taken for the two TCT airfoils at low and high lift conditions, respectively, FIG. 6, one notes that the large differences in lift at a given angle-of-attack are mainly caused by differences in the upper surface shock locations and rear pressure distributions. It seems that, while the pressure distribution on the lower surface is not at all affected, the shock on the upper surface is pulled towards the leading edge due to the interaction of the airfoil flow field with the sidewall boundary layer.

FIG. 7 presents on the left a summary of the deviation from linearity determined from the lift results shown in the previous figure. The deviation parameter, ΔC_{LL}, as shown in the small insert sketch, represents the lift increment at a given angle-of-attack between the actual lift and a linear lift slope variation established by the low lift values. It will be noted again that the small chord TCT model and the CFWT model having about the same aspect ratio, but different tunnel-height to model-chord ratios display about the same maximum deviation from linearity. The onset of the divergence from linearity, i.e., the incidence for incipient divergence, however, is different for these two model-wind-tunnel system, while there is close agreement in the incidence for the onset of non-linear lift between the CFWT and the large chord TCT airfoils which have about the same tunnel-height to model-chord ratios. These results suggest that, while the magnitude of the non-linear lift variation is primarily influenced by aspect ratio, the onset of the divergence is dependent on tunnel-height to model-chord ratio and the associated degree of lift-interference effects. The filled triangular symbols reflect data obtained with the small chord TCT model while applying sidewall boundary layer suction amounting to 2% of the tunnel mass flow. The increase in the non-linear lift value, although small, supports the premise that the three-dimensional effects caused by the interaction of the model flow field with the sidewall boundary layer influence the overall flow development of the model-tunnel system in this range of lift coefficients. Results concerning sidewall BLC in the 0.3-m TCT have been reported in REF.9 for the NASA SC(3)0712 supercritical airfoil. Documentation of the CAST 10-2 sidewall BLC study is in progress.

At the right of this figure the maximum non-linear lift parameters, $(\Delta C_{LL})_{max}$, determined at M_∞ = 0.765 and Re = 10 x 10^6 are plotted as a function of model aspect ratio, AR (B/c). One data point, the diamond symbol, has been added here to indicate results obtained with a 1.7 aspect ratio airfoil in the DFVLR Transonic Wind Tunnel Braunschweig (TWB). If it is assumed that the maximum deviation from linearity parameter provides an indication of the extent of three-dimensional wall effects, these results suggest a leveling off of wall effects for aspect ratios above about 2.0. This value in aspect ratio is in close agreement with the conclusion from other investigations [7].

In the preceding discussion we addressed some of the major effects of the model-wind-tunnel system on wall interference effects at a given Reynolds number. Let us now turn briefly to the related subject and examine the effects of Reynolds number on (a) the actual airfoil aerodynamic characteristics associated with the non-linear lift behavior, and (b) the degree of the sidewall interference effects on the model flow field. The variation of the maximum non-linear lift-parameter, $(\Delta C_{LL})_{max}$, with Reynolds number has been selected to illustrate these effects. In FIG. 8 data are shown for the two TCT airfoils and the CFWT model at a constant Mach number over a Reynolds number range varying from about 4 to 30 million. Note, that the data shown for the Re = 4 x 10^6 case were selected from fixed transition results to avoid any erroneous conclusion due to "unstable" shifts in the point of boundary layer transition.

A review of these results indicates that for all three model-tunnel systems the maximum non-linear lift parameter is reduced with increasing Reynolds number. This trend suggests that the non-linearity is, at least in part, influenced by the viscous-inviscid interaction on the airfoil. In addition to starting at a much lower value of non-linear lift, the Reynolds number dependence for the low aspect ratio (B/c = 1.33) model-tunnel system, shown by the circular symbols, is appreciably less than for the higher aspect ratio model-tunnel configuration. This example provides a good illustration as to how pure Reynolds number effects can be obscured by the complex interaction between the model flow field and the boundary layer development on the test section sidewalls.

The attention given thus far to the non-linear lift characteristic of this class of airfoil might be considered to be somewhat academic. However, a thorough understanding of this development, eventually leading to the flow break-down, and its relationship to the effects of the model-tunnel system and Reynolds number is essential in the overall assessment of actual airfoil performance at the simulated flight equivalent conditions.

Let us consider a second example: When the Reynolds number is increased, the boundary layer developing on the sidewalls will become thinner if left "undisturbed". It might be expected then that shock induced sidewall boundary layer separation would be delayed for the "thinner" boundary layers at the higher Reynolds number thereby decreasing the resulting three-dimensional effects.

In FIG. 9 we have illustrated the effects of Reynolds number on the spanwise drag variation parameter, ΔC_{DL}, for the large and the small TCT models. The spanwise drag parameter as defined in the insert sketch, represents the difference between the drag levels measured at the tunnel centerline and a station midway between the centerline and the tunnel sidewall. As shown here, the drag variation across the tunnel at low angles-of-attack, prior to the onset of any significant non-linear lift effects, is small and virtually independent of model-tunnel system and Reynolds number effects. At an angle-of-attack of 3.5 degrees, however, at a condition which is well into the range of non-linear lift effects, there is not only the noticeable influence of the aspect ratio, but also a somewhat unexpected increase in spanwise drag variation with increasing Reynolds number. The latter may be related to the downstream movement of the airfoil upper surface shock and the increased shock strength at the higher Reynolds number. This illustration cites an example where the thinner sidewall boundary layer, at conditions which might be expected to be more stable and resistant to disturbance, may actually increase three-dimensional effects by promoting a more severe interaction between the tunnel sidewall and the airfoil flow field.

Maximum lift and drag rise

We have discussed in some detail the complex relationship between the aerodynamic behavior of the airfoil and the sidewalls of the model-tunnel system. In order to provide additional understanding regarding the related effects of model-tunnel systems and Reynolds number, let us now examine other characteristics, such as maximum lift and the drag divergence Mach number, which may be strongly influenced by the effects of the floor and ceiling of the test section.

At the left of FIG. 10, the maximum lift coefficient, C_{Lmax}, is plotted as a function of Mach number for the large and small chord TCT models and the Lockheed CFWT model at a Reynolds number of 10 million. It will be noted that there is a pronounced difference in the maximum lift values, particularly at the higher Mach numbers. These results suggest that there is a significant difference in the effective freestream Mach numbers for the various model-tunnel configurations considered.

This is confirmed by the results at the right of the figure where the drag coefficients determined at C_L = 0.50 and a Reynolds number of 10 million are plotted as a function of Mach number for the same three model-tunnel systems. There is a pronounced difference in the drag-rise Mach numbers between the TCT H/c = 4 and H/c = 8 configurations while there is a closer agreement between the TCT and CFWT H/c = 4 results. This suggests that there is a prevailing influence of the tunnel-height to model-chord ratio on the aerodynamic characteristics considered here. That the causes for the differences in maximum lift and the drag-rise Mach number are of the same origin is substantiated by empirically correcting the Mach numbers for maximum lift at constant maximum lift by the difference in drag-rise Mach number relative to the small-chord TCT model. This correction results in a surprisingly good correlation in the maximum lift results shown in the left figure by the half-filled symbols. However, it must be noted that at higher lift coefficients this empirical procedure gives less satisfying, although qualitatively correct, results.

Having reviewed examples of the primary effects of wind-tunnel walls on the maximum lift and drag rise characteristics, let us now consider the effects of Reynolds number on the same parameters. In FIG. 11 the maximum lift determined at a Mach number of 0.765 is plotted as a function of Reynolds number for the same model-tunnel systems just discussed. In addition results are shown at relatively low Reynolds numbers which were obtained in the DFVLR-TKG facility. The open symbols indicate transition free results, the half closed symbols show transition fixed data. The comparison again vividly demonstrates the dominant influence of the model-wind-tunnel system on the maximum lift parameter with the small height-to-chord ratio airfoils displaying the highest values of maximum lift. All of the model-tunnel configurations exhibit an increase in maximum lift with increasing Reynolds number up to the highest conditions investigated. However, there is an interesting difference in the rate of increase with Reynolds number between the various model-tunnel set-ups. The two models in the slotted TCT display a similar gradient; the results obtained in the perforated CFWT and TKG tunnels are similar to each other but reflect a higher rate of change with Reynolds number. Since the free and fixed transition results show about the same dependence on Reynolds number, it is unlikely that differences in the transition fixing devices caused any significant change in the Reynolds number dependence of maximum lift. It can be assured then, that the difference noted in the family of slopes for the slotted and perforated tunnels is due to the effect of Reynolds number on the degree of wall interference effects.

Turning to the second characteristic parameter, FIG. 12 presents the variation of the drag-rise Mach number at $C_L = 0.50$ with Reynolds number for the two TCT models and the CFWT model. As in the case of the preceding maximum lift example, there is a pronounced difference in the Reynolds number dependence of the drag-rise Mach numbers determined for the TCT models and the CFWT model-tunnel system. For the TCT configurations, a slight decrease in the drag-rise Mach number is exhibited with increasing Reynolds number. An opposing trend is displayed for the CFWT airfoil, which shows a noticeable increase in the drag-rise Mach number with increasing Reynolds number. If it is assumed that the TCT results for these conditions represent the proper Reynolds number dependence, the increase in the drag-rise Mach number would suggest that the effective freestream Mach number in the CFWT decreases with increasing Reynolds number. If this assumption were correct, it would mean that the wind-tunnel walls behave in a more "open" fashion with increasing Reynolds number. This is supported by the previously shown results which indicated a much higher rate of increase in the maximum lift coefficient with Reynolds number for the CFWT model. It will also be noted here that the two TCT systems show about the same Reynolds number dependence even though there is a great difference in the aspect ratios, B/c, which substantiates that the differences in the drag-rise characteristics discussed here are primarily caused by the influence of the floor and ceiling and the associated effects of Reynolds number.

Both, the drag-rise Mach number and the maximum lift coefficients reflect differences due to changes in Mach number which occur as a result of undesirable model-tunnel wall interference effects. The unknown regarding Mach number can be eliminated by combining the drag rise and maximum lift parameters into a new parameter, the maximum lift at drag rise, $(C_{Lmax})_{M_{\infty D}}$. In FIG. 13 the maximum lift at drag rise parameter is plotted as a function of Reynolds number for the two TCT and the CFWT model-tunnel systems. A review of the results indicates that when the maximum lift and drag rise characteristics are combined in this manner, all three model-tunnel systems exhibit essentially the same degree of dependence on Reynolds number. The slight scatter in the data is within the lift accuracy requirements quoted by an AGARD Conveners Group on "Data Accuracy and Flow Quality Requirements in Wind Tunnels"[10]. These results provide a strong indication that for some wind tunnels, the Reynolds number dependence of certain aerodynamic parameters are, indeed, due in part to the influence of Reynolds number on the wall characteristics. In comparing the results for the TCT and CFWT tests it appears that perforated wall tunnels are much more susceptible to Reynolds number effects than slotted wall tunnels. It must, furthermore, be realized that it is not possible to eliminate this "pseudo" Reynolds number effect by simply calibrating the empty tunnel over the unit Reynolds number range of the facility. The actual flow characteristics of the partially open walls over the desired Reynolds number range must be determined but this represents a very rigorous process and does not always guarantee success. The only feasible way, short of adaptive walls, then seems to be to determine the wall boundary conditions as input to a suitable wall interference correction method. It must be stressed that actual Reynolds number effects on the airfoil flow development can only be determined after the proper elimination of the wall interference effects at all conditions.

"PURE" REYNOLDS NUMBER EFFECTS

The third and final portion of this paper will deal with the interference-free Reynolds number effects on the aerodynamic characteristics of the airfoil. Although the wall interference effects of the various model-tunnel systems cannot be ignored completely, they will only be considered in this portion of the paper to enable an analysis of the interference-free trends in the aerodynamic characteristics.

The angle-of-attack necessary to establish a given lift coefficient provides a good indication of the sensitivity of an airfoil to Reynolds number changes as well as of the difference in lift interference effects between the various model-tunnel systems. In FIG. 14 (a), the angle-of-attack required to produce a lift coefficient of $C_L = 0.55$ at a Mach number of 0.765 is plotted as a function of Reynolds number for the two TCT and the CFWT models. The transition fixed and the high Reynolds number results show a steady decrease in the incidence for $C_L = 0.55$ up to the highest Reynolds number investigated. Considering fixed transition, the difference in the incidence angle at $Re = 4 \times 10^6$ between the H/c = 4 airfoils and the H/c = 8 TCT model is 0.5 degrees. This change in

incidence is reduced to about 0.36 degrees at a Reynolds number of Re = 40 x 10^6. The very small change in the incidence angle between these Reynolds number extremes may be related to wall interference effects. However, since this slight difference in angle-of-attack corresponds to a change in lift coefficient of only about 0.025, which is close to the desired lift accuracy requirement of ±0.01 [10], characteristic trends noted here and in the following figures can be considered to represent the "interference-free" Reynolds number effects on the airfoil characteristics. Note, that in the case of low Reynolds number free transition the differences in incidence for C_L = 0.55 between the respective model-tunnel configurations can not be reproduced. This is likely to be due to different transition point locations caused by the various levels of turbulence and model roughness for the different model-tunnel systems.

In FIG. 14 (b), results obtained in the DFVLR TKG and TWB facilities have been added to the angle-of-attack for constant lift results shown in the preceding figure. The TCT and CFWT turbulent boundary layer trends have been summarized here and are indicated by two lines. Both, the TKG and TWB results exhibit essentially the same trends in Reynolds number dependence as was determined in the TCT and CFWT facilities. It is clearly indicated by the large incidences shown for the TKG facility that the 6-percent open, perforated test section [4] is much too open for interference free testing. The TWB with a tunnel-height to model-chord ratio of only 3 produces results which are close to the results shown for the H/c = 8 TCT system. The TWB facility has slotted walls with an open area ratio of about 2.4 percent which have been optimized for zero blockage [5]. The TWB results suggest that the wall interference effects can be significantly reduced by properly ventilating the tunnel walls even in situations where the tunnel-height to model-chord ratios might be considered unacceptably low.

Following the preceding discussion, FIG. 15 (a) then summarizes the "pure" effects of Reynolds number at a Mach number of 0.765 on lift at a given angle-of-attack for five different CAST 10-2 model-tunnel systems. The incidence angles, shown in the key for each model-tunnel set-up, were selected to provide about the same lift coefficient at Re = 10 x 10^6, transition fixed. When this procedure was followed, all of the transition fixed results fell within a relatively narrow band which corresponds to an accuracy in lift coefficient of about ± 0.01. With turbulent boundary layer conditions, i.e., either fixed transition or free transition at Re > 10 x 10^6, the lift coefficients increase throughout the entire Reynolds number range extending from about 1.9 to 40 million. The total change in lift between these Reynolds number extremes is significant and amounts to an increment in C_L of about 0.20 or 33 percent of the lift value at Re = 40 x 10^6. This rather dramatic increase in lift is believed to be due to changes in the initial displacement thickness (fluid shape of the airfoil) with increasing Reynolds number and the resulting condition of the flow leaving the trailing edge of the airfoil [1]. This assumed effect is further demonstrated by the lift behavior of the transition free results determined at the lower test Reynolds numbers. The transition point is initially far "downstream" resulting in a thin boundary layer and a correspondingly high lift coefficient. As the Reynolds number is increased, the transition point moves forward on the airfoil increasing the displacement thickness and, in turn, reducing the lift coefficient. This progression continues and slowly diminishes with increasing Reynolds number until the point of transition has reached a stable, nearly fixed position, close to the leading edge of the airfoil. The large differences in the low Reynolds number transition free results indicate a high susceptibility of the flow development to characteristics associated with the various model-tunnel systems such as wind tunnel noise, turbulence and model roughness.

This summary suggests that it would be difficult to extrapolate the free transition results for this airfoil to full-scale conditions even if data were available up to a Reynolds number of Re = 30 x 10^6. In the case of the fixed transition results where the progression of lift with Reynolds number is more systematic, an extrapolation from low to high Reynolds numbers seems possible; however, before reaching a general conclusion let us examine first the next figure.

FIG. 15 (b) illustrates the dependence of lift on Reynolds number for a second set of test conditions. Here, lift results are shown for the H/c = 4 TCT and CFWT model-tunnel systems at a Mach number of 0.75 and an angle-of-attack of $\alpha \approx 3$ degrees. The lift behavior at the lower Reynolds numbers is very similar to the results shown in the preceding figure; however, at Reynolds numbers between 10 and 20 million a reversal occurs in the Reynolds number dependency. It is obvious from this illustration that an extrapolation of low Reynolds number results to flight conditions would be impossible. This reversal, as revealed by the pressure distributions of FIG. 16, is caused by an "irregular" behavior of the upper surface shock which either ceases to move downstream or shifts upstream with increasing Reynolds number, FIG. 16 b and 16 c. The phenomenon is not yet completely understood, although some indication might be obtained from the CFWT results. Since the trailing edge pressure continues to increase with Reynolds number, it appears that here the local effects due to a reduction in displacement thickness override the global effects associated with changes in the flow conditions at the trailing edge of the airfoil. It is worthwhile noting that both of the H/c = 4 TCT and CFWT model-tunnel systems reflect this type of lift dependence on Reynolds number.

Airfoil performance is always a subject of major interest to the aerodynamicist. This presentation therefore will be concluded with what is considered to be the interference free variation of the well known aerodynamic range parameter $(C_L/C_D \cdot M_\infty)_{max}$ with Reynolds number, the latter extending here from ambient wind tunnel to flight equivalent conditions for large transport class aircraft,FIG. 17. Since this particular performance parameter is highly dependent upon the drag levels near the drag-rise Mach number, the empirical Mach number correction discussed earlier in this paper has been applied to the results for the three larger, i.e., H/c = 4 and 5, airfoil models. The adjusted results for the four model-tunnel systems exhibit a good agreement in the variation of the range parameter with Reynolds number. It is also interesting to note the surprisingly large variation in performance over the Reynolds number range of the tests which amounts to an increase in the range parameter of about 45 percent based on the value at Re = 40 x 10^6. Here again, these results clearly indicate the difficulty in extrapolating performance data based on low Reynolds number characteristics.

It will be noted that there is a slight decrease in the range parameter at Reynolds numbers between 30 and 40 million which is due to a drag increase in this Reynolds number range. The exact reason for this drag increase has not yet been established, but it does serve to illustrate the importance of testing at, and possibly slightly beyond, the design and off-design flight equivalent conditions. The ability to test at the high Reynolds number conditions, furthermore, enables experimental studies of complex basic phenomena, such as for instance shock boundary layer interactions, which cannot be modeled accurately with current theroretical methods.

IV CONCLUSIONS

An extensive study has been made of the CAST 10-2/DOA2 transonic airfoil in both ambient temperature and advanced cryogenic temperature wind tunnels at transonic Mach numbers over a large range of Reynolds numbers including flight equivalent conditions. The initial analysis of the extensive CAST 10-2 airfoil results has led to the following conclusions:

1. Certain classes of supercritical airfoils may exhibit a non-linear increase in lift which is at least in part related to viscous-inviscid interactions on the airfoil. This non-linear lift characteristic can be erroneously suppressed by wall interference effects in addition to being affected by changes in Reynolds number.

2. Wind tunnel wall interference effects can be severe and completely overshadow a determination of the actual airfoil aerodynamic characteristics. Moreover, the degree of wall interference effects can be significantly affected by changes in Reynolds number, thus appearing as "true" Reynolds number effects.

3. Two-dimensional airfoil models and wind tunnels must be considered as a complete and totally integrated system for which all boundary conditions must be obtained. This approach can enable the separation of the complex and interrelated effects of the tunnel walls and the actual aerodynamic characteristics of the airfoil.

4. "Real" Reynolds number effects on the CAST 10-2 airfoils have been determined and have been shown to be very appreciable. For instance, near the airfoil design condition, a 45 percent increase in the aerodynamic range parameter was observed when the Reynolds number was increased from 2 to 40 million.

5. For certain classes of airfoils, an accurate extrapolation of low Reynolds number results to flight equivalent conditions seems not possible, making at least research facilities operating beyond flight equivalent Reynolds numbers necessary.

The CAST 10-2 high Reynolds number results have provided new insight into the aerodynamic behavior of this class of airfoils and have provided a valuable aid in the analysis of wall interference and Reynolds number effects. There are still many questions left unanswered; however, the analysis of the data is continuing and the forthcoming tests in cooperation between NASA, ONERA and DFVLR in advanced adaptive wall facilities will provide additional knowledge regarding the complex problems associated with wall interference and "true" Reynolds number effects.

REFERENCES

1. Stanewsky, E., "Interaction between the outer inviscid flow and the boundary layer on transonic airfoils", Z. Flugwiss. Weltraumforsch. 7 (1983), Heft 4, pp. 242 - 252

2. Stanewsky, E. and Zimmer, H., "Development and wind tunnel test of three supercritical airfoils for transport aircraft", Z. Flugwiss. 23 (1975), Heft 7/8, pp. 246 - 256

3. Hottner, Th. and Lorenz-Meyer, W., "The Transonic Wind Tunnel of the Aerodynamische Versuchsanstalt Göttingen", DGLR-Jahrbuch 1968, pp. 235 - 244

4. Stanewsky, E., Puffert-Meissner, W., Müller, R. and Hoheisel, H., "The Transonic Wind Tunnel Braunschweig of the DFVLR", Z. Flugwiss.Weltraumforsch. 6 (1982), Heft 6, pp. 398 - 408

5. Pounds, G.A. and Stanewsky, E., "The Research Compressible Flow Facility", Lockheed-Georgia Company Report ER-9219, 1967 (also see: Blackwell, J.A.,"Wind tunnel blockage correction for two-dimensional transonic flow", J. Aircraft, Vol.16, No.4, 1979)

6. Ray, E.J., Ladson, C.L., Adcock, J.B., Lawing, P.L. and Hall, R.M., "Review of design and operational characteristics of the 0.3-m Transonic Cryogenic Tunnel", NASA TM-80123, Sept. 1979

7. Elsenaar, A. (Editor), "Two-dimensional transonic testing methods", GARTEur/TP-011, 1983 (Final report of the GARTEur Action Group AD (AG 02))

8. Kemp, W.B., "TWINTAN: A program for transonic wall interference assessment in two-dimensional wind tunnels", NASA TM-81819, May 1980

9. Murthy, A.V., Johnson, C.B., Ray, E.J.,Lawing, P.L. and Thibodeaux, J.J., "Investigation of the effects of upstream sidewall boundary-layer removal on a supercritical airfoil", AIAA 21st Aerospace Sciences Meeting, Reno, Nevada, January 10-13, 1983, Paper No.83-0386

10. Steinle, F. and Stanewsky, E., "Wind tunnel flow quality and data accuracy requirements", AGARD Advisory Report No. 184, Nov. 1982

TABLE 1: CAST 10-2 airfoil studies

TUNNEL	MODEL CHORD (mm)	TUNNEL CHARACTERISTICS				TEST CONDITIONS			
		H/c	B/c	TYPE WALL	POROS. σ %	M_∞	α°	Re x 10^{-6}	TRANSITION
TKG	200	5	5.0	Perf.	6	0.50 ÷ 0.82	-2÷10	1.3÷ 4	Fixed & Free
TWB	200	3	1.7	Slotted	2.4	0.6;0.7;0.76	↓	3÷14	↓
CFWT	178	4	2.9	Perf.	4	0.60 ÷ 0.82		4÷31	
0.3-m TCT[1]	152	4	1.33	Slotted	5	0.60 ÷ 0.80 ↓		4÷45	
0.3-m TCT[1]	76	8	2.66	Slotted	5			4÷20	
T2 0.3-m TCT TKG,TWB	ONERA and NASA streamlined wall tests and additional DFVLR tests (1984)								

[1]with/without BLC

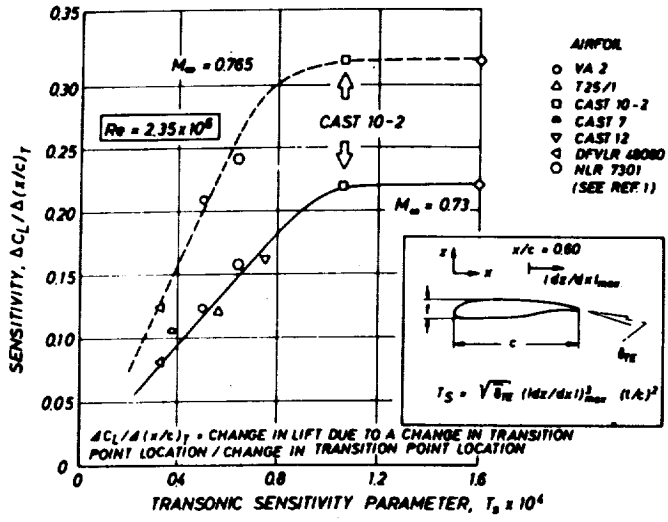

FIGURE 1: Flow sensitivity to changes in the initial boundary layer condition (from REF. 1)

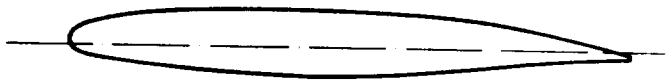

FIGURE 2: CAST 10-2/DOA2 characteristics

AIRFOIL CHARACTERISTICS : $t/c = 0.121$ at 45% c
$(t/c)_{TE} = 0.005$

THEORETICAL DESIGN POINT : $M_\infty = 0.76$, $C_L = 0.595$
$\alpha = 0.3°$

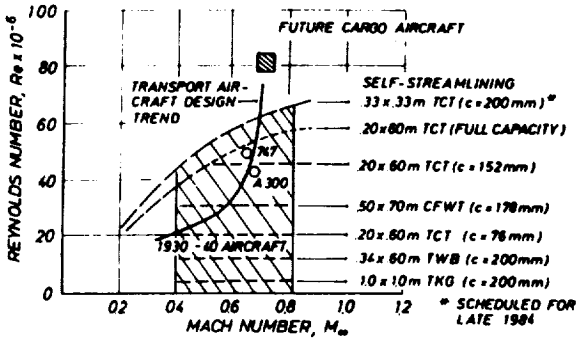

FIGURE 3: CAST 10-2/DOA2 test envelopes

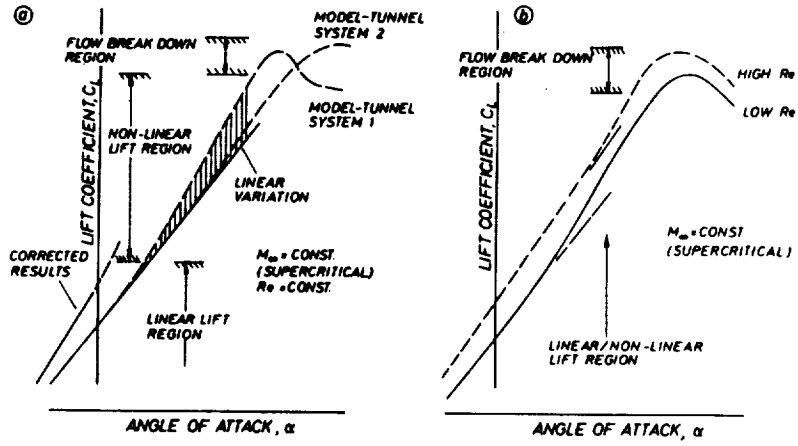

FIGURE 4: Effect of ⓐ model-wind-tunnel system and ⓑ Reynolds number on lift behavior (schematic)

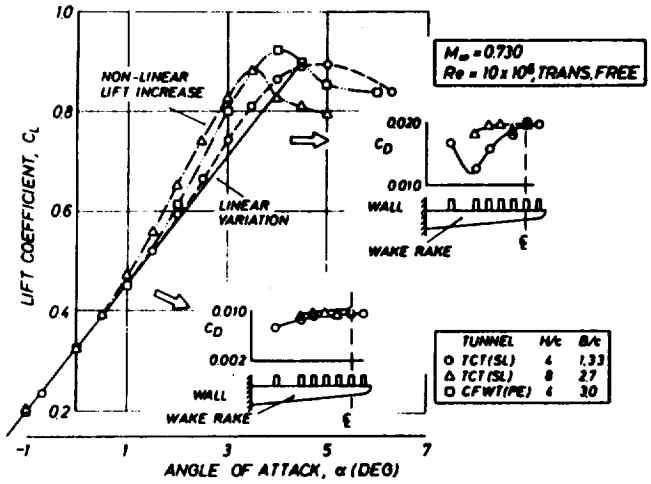

FIGURE 5: Tunnel (side) wall effects on lift increase with angle-of-attack

FIGURE 6: Tunnel (side) wall effects on the chordwise pressure distribution (test cases of FIG.5)

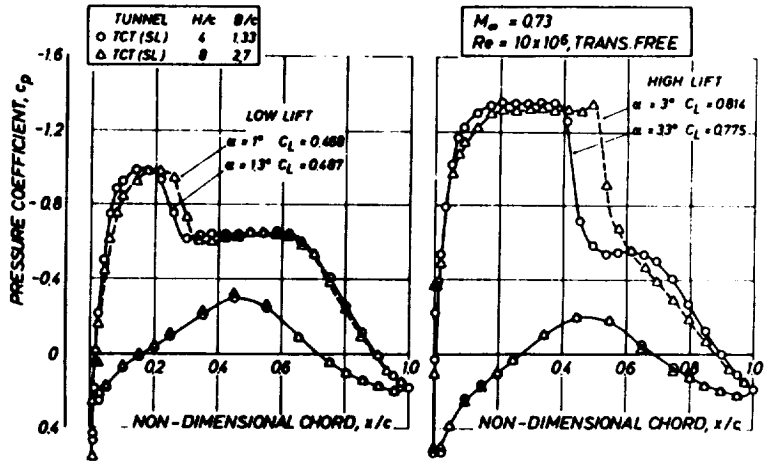

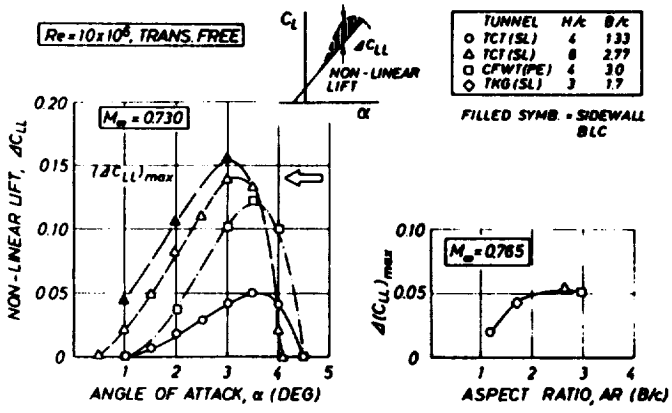

FIGURE 7: Effect of aspect ratio on the deviation from lift linearity

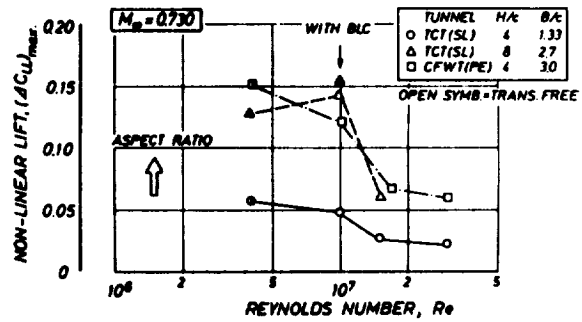

FIGURE 8: Reynolds number effects on maximum lift non-linearity

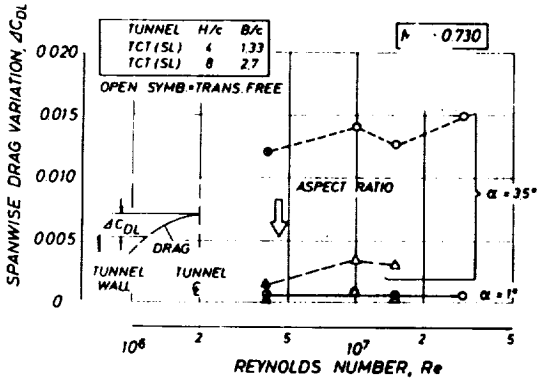

FIGURE 9: Reynolds number effects on spanwise drag variation

FIGURE 10: Wall interference effects on maximum lift and drag

(↓ Indicates $M_{\infty D}$)

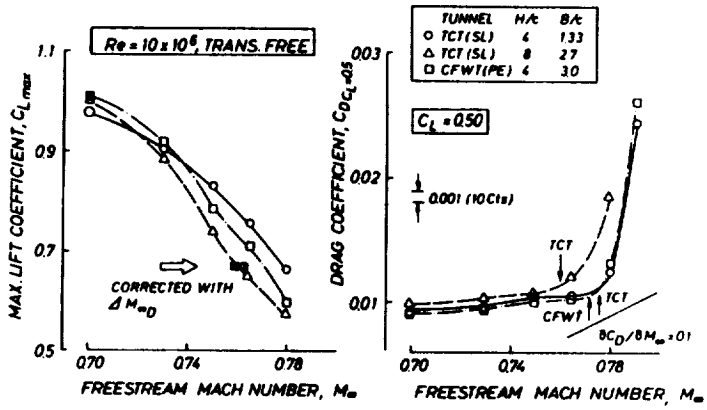

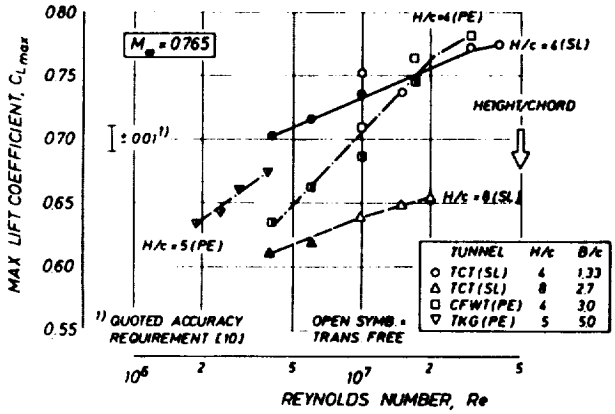

FIGURE 11: Effect of Reynolds number and model-wind-tunnel system on maximum lift

FIGURE 12: Effect of Reynolds number and model-wind-tunnel system on the drag-rise Mach number

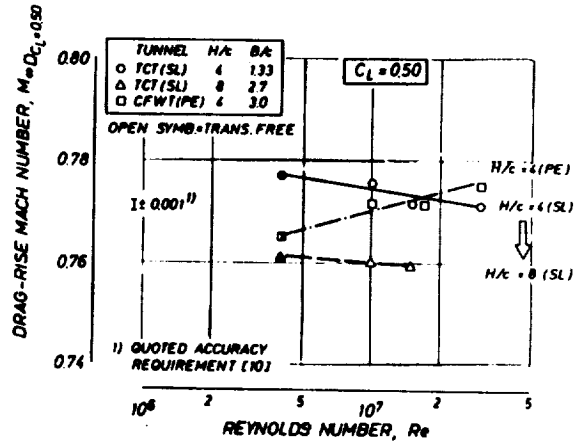

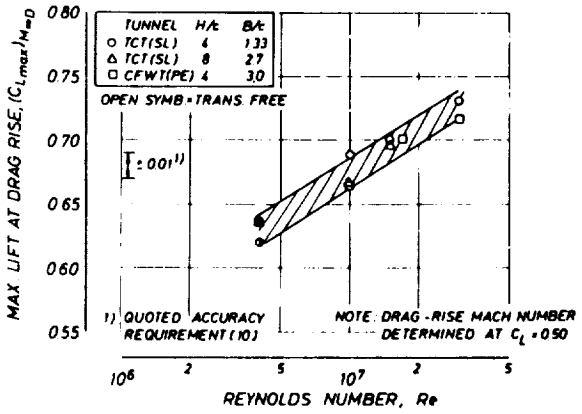

FIGURE 13: Effect of Reynolds number on the maximum lift at drag rise

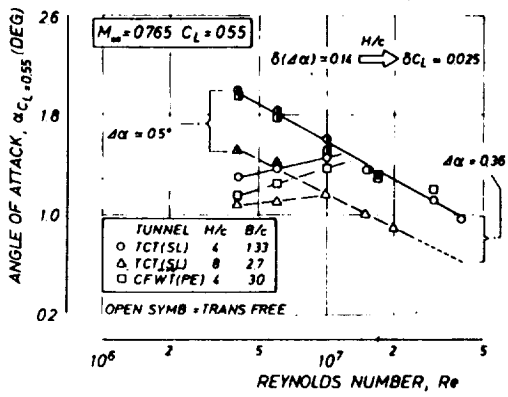

a. 0.3-m TCT and CFWT model-wind-tunnel configurations

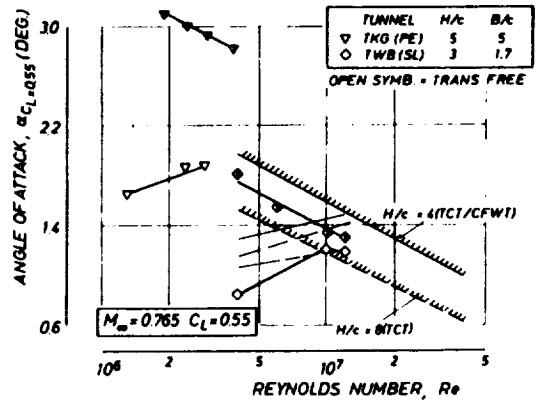

b. TWB and TKG model-wind-tunnel configurations

FIGURE 14: Reynolds number dependence of the angle-of-attack for constant lift

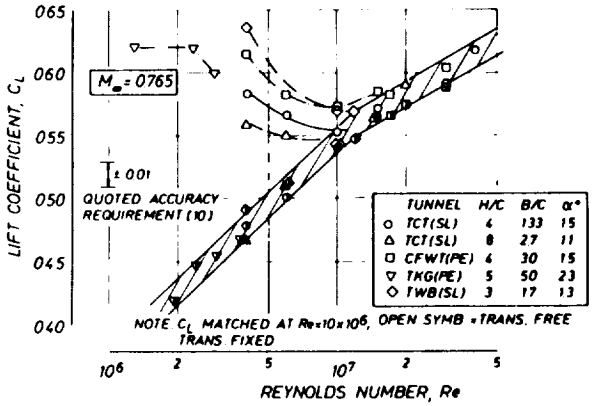

a. M_∞ = 0.765 α = const.

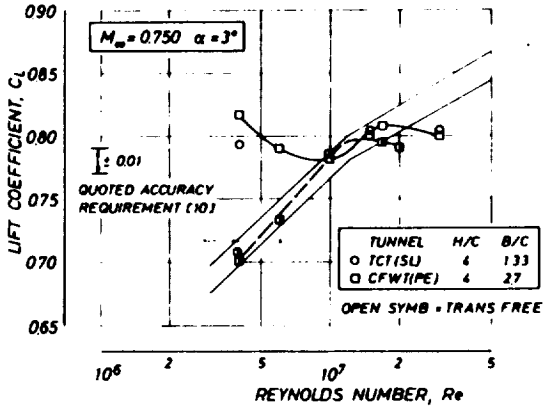

b. M_∞ = 0.750 α = const.

FIGURE 15: Effect of Reynolds number on lift

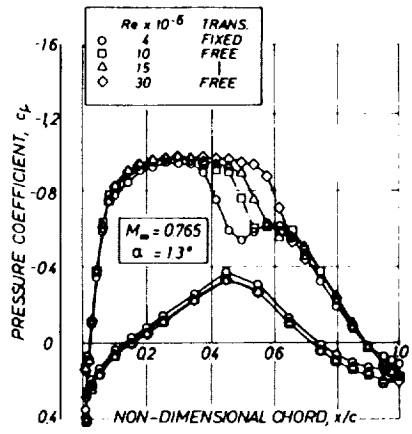

a. M_∞ = 0.765 α = 1.3° TCT-results

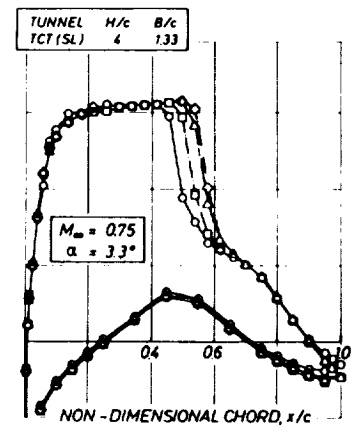

b. M_∞ = 0.750 α = 3.3° TCT-results

FIGURE 16: Effect of Reynolds number on pressure distribution (test cases of FIG. 15)

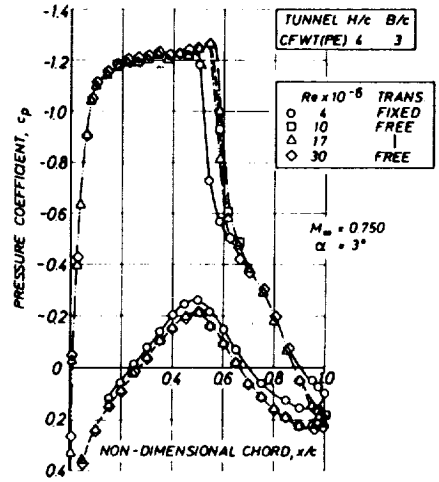

c. M_∞ = 0.750 α = 3° CFWT-results

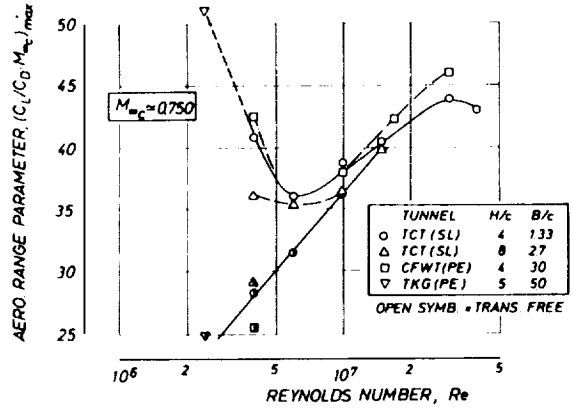

FIGURE 17: Effect of Reynolds number on the aerodynamic range parameter